Patricia Butler, Ali Vahdati, PhD, Stacey Meardon, PhD, Stephanie George, PhD
Department of Engineering and Department of Physical Therapy

Cost-Benefit Analysis of 3D FE Modeling of the Tibia Throughout the Stance Phase

Background

Bone Stress Injuries (BSIs)

- Can be caused by repetitive forces from running [1]
- 40-60% of BSIs occur in the tibia [2]

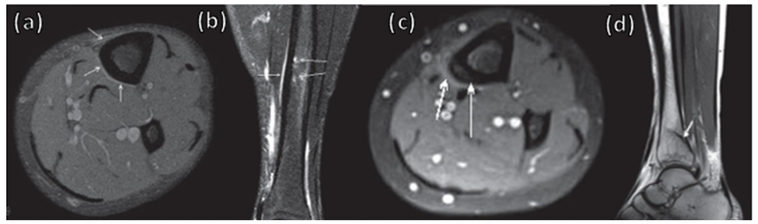

Figure 1: MRIs of BSIs with increased grading scales defined by Gmachowska et al. [3]. (a) Grade 1 with periosteal edema (b) Grade 2 with bone marrow and periosteal edema (c) Grade 3 with cortical abnormalities, bone marrow and periosteal edema (d) Grade 4 with a fracture line. Images adapted from [3].

Computational Models

3D Models	2D Cross-Sections
	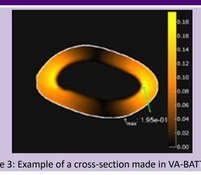
Figure 2: Example of a 3D model created in Mimics and 3-Matric.	Figure 3: Example of a cross-section made in VA-BATTS [4].

Objectives:

1. Find the differences between the FEA results in 3D models and 2D cross-sectional models
2. Identify if these differences are clinically significant
3. Determine limitations in each method

Data Collection

Collection of Kinetic/Kinematic Data

Figure 4: Subjects warmed up on an instrumented force treadmill (Bertec, Columbus, Ohio, USA) [5].

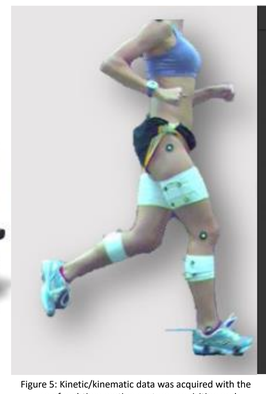

Figure 5: Kinetic/kinematic data was acquired with the use of real-time motion capture acquisition and processing software. Reflective markers were tracked with a 10-camera 3D motion capture system [6].

Figure 6: Ground reaction forces were filtered, kinetic/kinematic data from the stance phase was isolated, and the isolated data was used in a musculoskeletal model to approximate the muscle forces at the location of interest. Image modified from [7].

- Finally, static optimization and vector summation was performed with the distal tibia reaction forces and muscle forces to estimate the forces affecting the distal tibia

MR Image Acquisition

- MR images were collected of the frontal, coronal, and sagittal plane of the subject's right tibias with a 1.5-T scanner with a torso coil
- Vitamin E capsules were used to assist with aligning the coordinate system

FEA on 3D Models

Creating and Meshing 3D Models

Generating Models (in Mimics and 3-Matic):

- Semiautomatic segmentation
- Wrapped and smoothed
- Inner bone subtracted from entire bone

Orientation (in Mimics and 3-Matic):

- Defined centroids used to determine current/desired orientations
- Rotated/translated model as needed

Trimming (in 3-Matic):

- Trimmed models at the distal 15% and proximal 85%

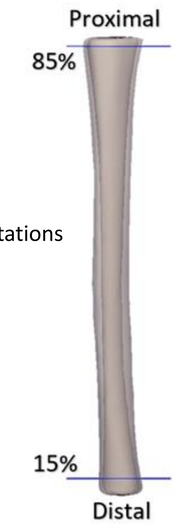

Figure 7: Representation of trimming 3D models.

Performing FEA in ANSYS Mechanical:

Material properties:

- Young's modulus: 17.19 GPa | Poisson's ratio : 0.3 [8]
- Ran FEA at each 10% of the stance phase

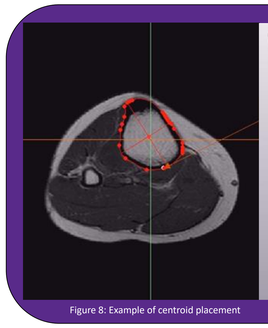

Figure 8: Example of centroid placement

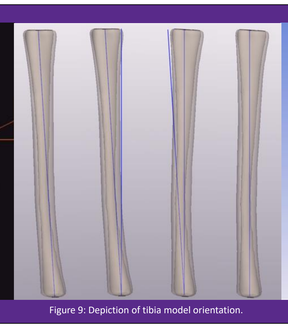

Figure 9: Depiction of tibia model orientation.

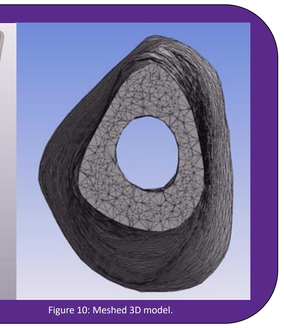

Figure 10: Meshed 3D model.

FEA on 2D Cross-Sections

Using VA-BATTS [4]

Adapting for MR images:

- Uniform Young's Modulus
- Polygon Fit
- Inverted and Rotated Image

Solving for Strains:

- Young's Modulus: 17.19 GPa [8]
- Hooke's Law:

$$\varepsilon = \frac{\sigma}{E}$$

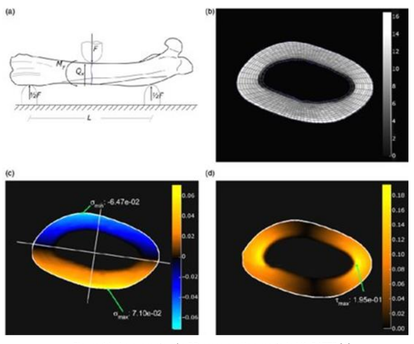

Figure 11: An example of a 2D cross-section made in VA-BATTS [4].

Acknowledgements

Funding from the National Science Foundation EEC-1359183 and the ECU Graduate School; John Wilson, PhD, MPT; Richard Willy, PhD, PT, OCS; Mara Thompson.

Results/Discussion

Results

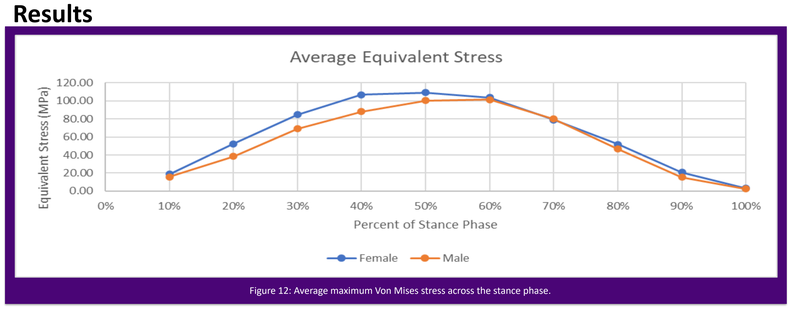

Figure 12: Average maximum Von Mises stress across the stance phase.

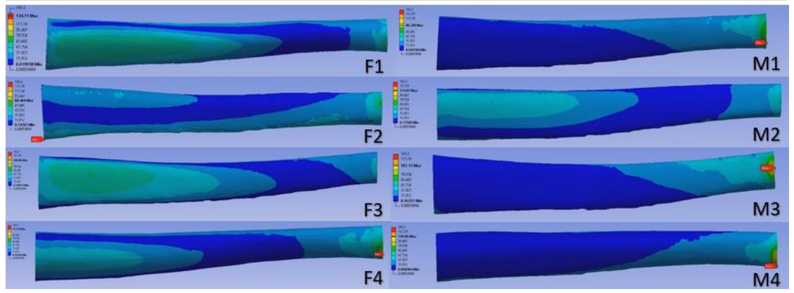

Figure 13: Maximum Von Mises stress distribution for all participants.

Table 1: Averaged maximum values Throughout the stance phase.

Metric	All	Males	Females	Published Values
Max Von Mises Stress (MPa)	104.76 ± 16.59	101.21 ± 9.35	109.33 ± 19.34	102.1 (Male) 120.24 (Female) [9]
Max Von Mises Strain (με)	6100.31 ± 965.33	5897.58 ± 542.31	6361.60 ± 1123.37	7939.79 ± 1588.74 [8]
Max Normal Strain (με)	3684.91 ± 1284.91	4085.38 ± 1260.31	3284.45 ± 1180.19	Max Compressive Strains: 2800-4800 [10]

Discussion

- Average maximum equivalent stress/strain occurred towards the middle of the stance phase
- Variances between collected values and published values could be due to differences in methodology or subject populations such as:
  - [9] included trabecular and cortical bone and only used a male and a female
  - [8] did not use subject specific models
  - [10] only used male models
- Study Limitations: small population size, cortical bone-only hollow models, and a generalized Young's modulus
- Next Steps: Analyze 2D cross-sectional data and perform data analysis

References

1. Meardon, S. A., Willson, J. D., Gries, S. R., Kernozek, T. W., & Derrick, T. R. (2015). Bone stress in runners with tibial stress fracture. *Clinical Biomechanics*, 30(9), 895-902. doi:10.1016/j.clinbiomech.2015.07.012
2. Harrast, M. (2019). *Clinical Care of the Runner E-Book*. Philadelphia: Elsevier.
3. Gmachowska, A., Żabicka, M., Pacho, R., Pacho, S., Majek, A., & Feldman, B. (2018). Tibial stress injuries – location, severity, and classification in magnetic resonance imaging examination. *Polish Journal Of Radiology*, 83, 471-481. doi: 10.5114/pjr.2018.80218
4. Kourtis, L., Carter, D., Kesari, H., & Beaupre, G. (2008). A new software tool (VA-BATTS) to calculate bending, axial, torsional and transverse shear stresses within bone cross sections having inhomogeneous material properties. *Computer Methods In Biomechanics And Biomedical Engineering*, 11(5), 463-476. doi: 10.1080/10255840801930728
5. *MIE Medical Research Limited | Bertec Instrumented Treadmills*. Mie-uk.com. (2021). Retrieved 17 March 2021, from https://www.mie-uk.com/bertec/treadmills/index.html.
6. Meardon, S. (2020). Biomechanics and Stress Fractures: Utility of Running Gait Analysis. *Stress Fractures In Athletes*, 107-128. doi: 10.1007/978-3-030-46919-1_8
7. Arnold, E. M., Ward, S. R., Lieber, R. L., & Delp, S. L. (2010). A model of the lower limb for analysis of human movement. *Annals of biomedical engineering*, 38(2), 269–279. https://doi.org/10.1007/s10439-009-9852-5
8. Chen, T., An, W., Chan, Z., Au, I., Zhang, Z., & Cheung, R. (2016). Immediate effects of modified landing pattern on a probabilistic tibial stress fracture model in runners. *Clinical Biomechanics*, 33, 49-54. doi: 10.1016/j.clinbiomech.2016.02.013
9. Tarapoom, W., & Puttapitukporn, T. (2016). Stress Distribution in Human Tibia Bones using Finite Element Analysis. *Engineering Journal*, 20(3), 155-167. doi: 10.4186/ej.2016.20.3.155
10. Edwards, W., Taylor, D., Rudolphi, T., Gillette, J., & Derrick, T. (2009). Effects of Stride Length and Running Mileage on a Probabilistic Stress Fracture Model. *Medicine & Science In Sports & Exercise*, 41(12), 2177-2184. doi: 10.1249/mss.0b013e3181a984c4